Israel Journal of Chemistry

IJC

Official Journal of the Israel Chemical Society

REPRINT

www.ijc.wiley-vch.de

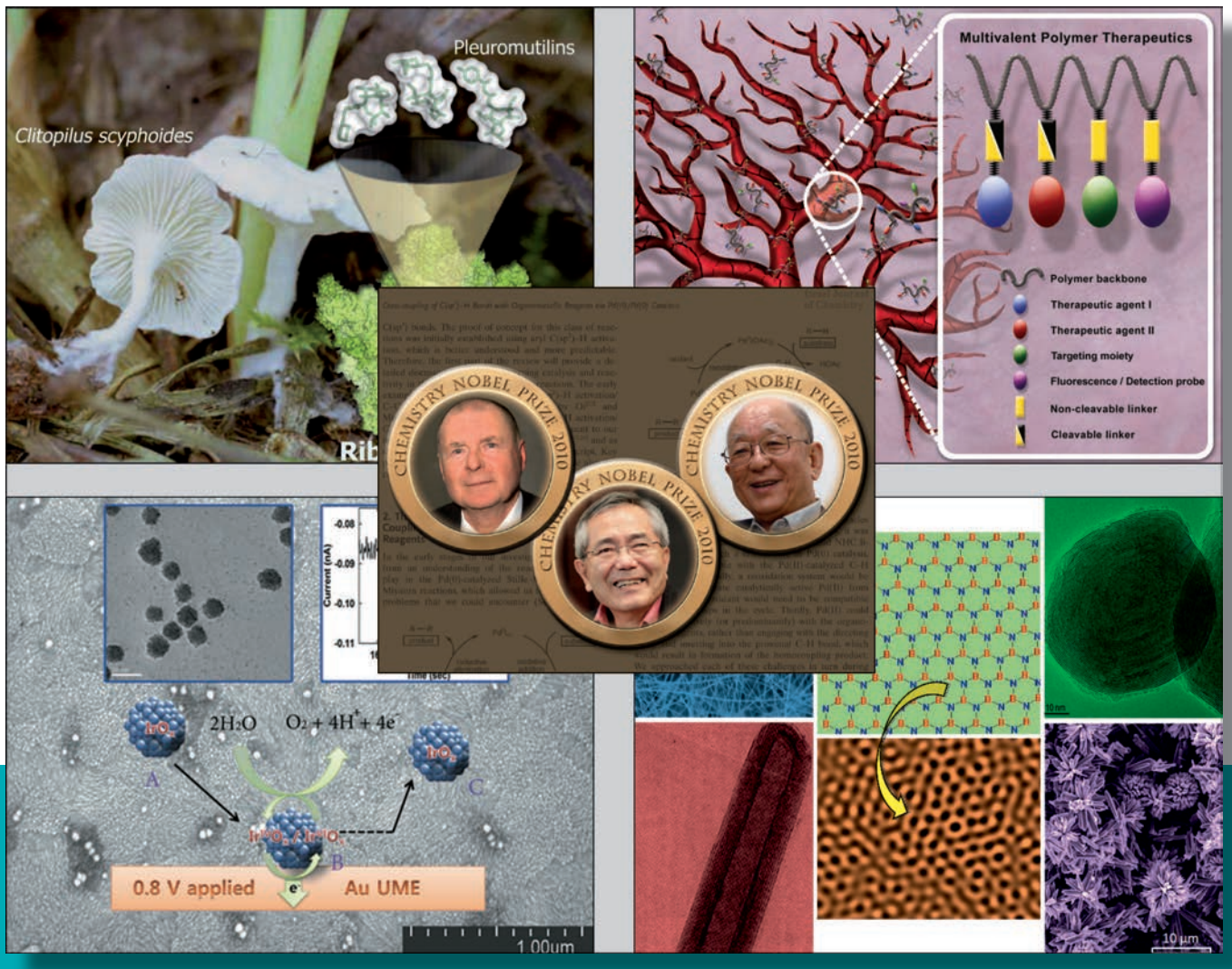

WILEY-VCH

Israel Journal of Chemistry

IJC

Official Journal of the Israel Chemical Society

Table of Contents

WILEY-VCH

ISJCAT 53 (6–7) 317–488 (2013) · ISSN 0021-2148 · Vol. 53 · No. 6–7 · June 2013

Israel Journal of Chemistry

IJC

Official Journal of the Israel Chemical Society

Contemporary Topics in Nucleic Acid Chemistry

Guest Editor: Yitzhak Tor

6–7/2013

www.ijc.wiley-vch.de

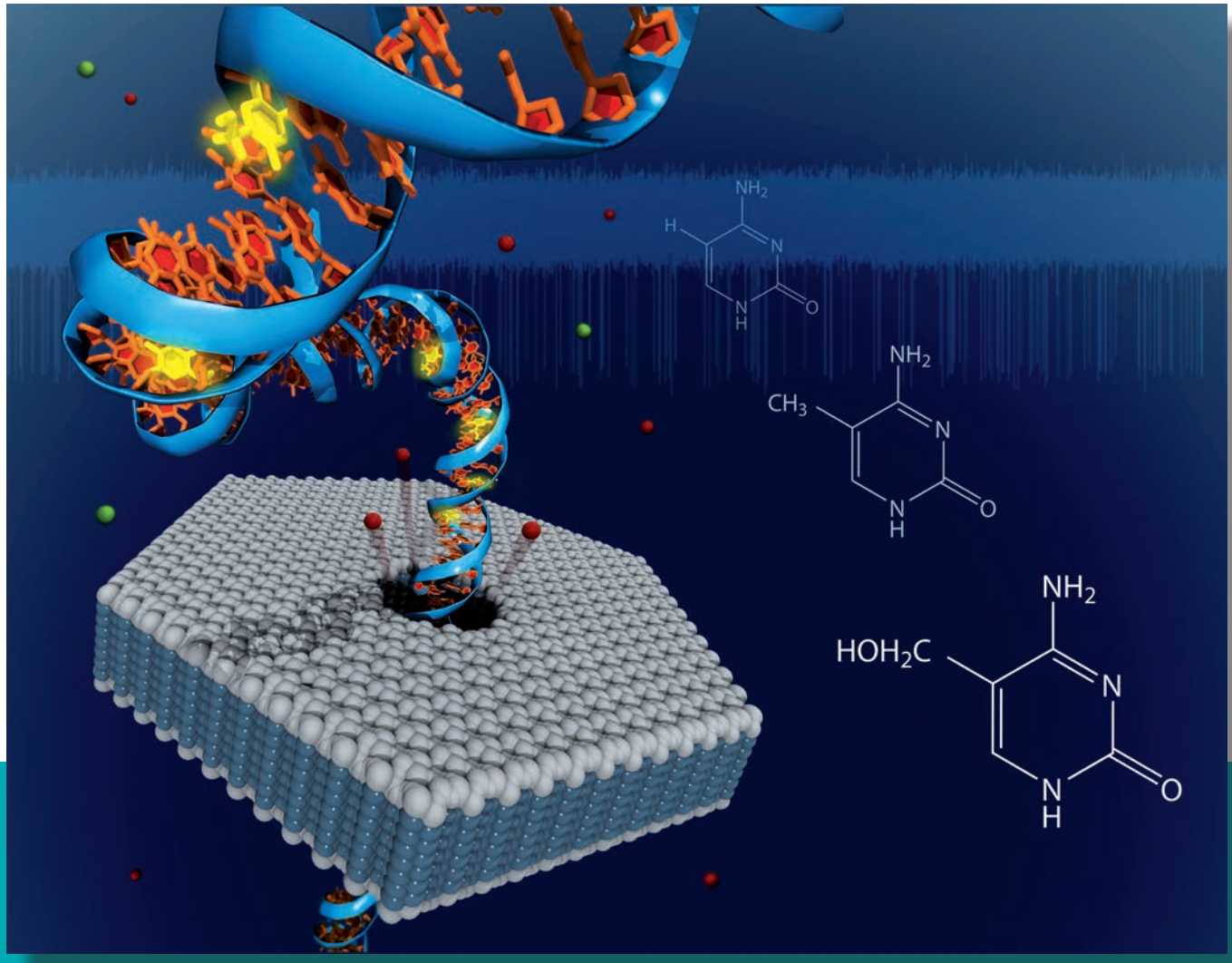

Volume 53

WILEY-VCH

Review

Israel Journal of Chemistry

DOI: 10.1002/ijch.201300006

Nanopore-Based Analysis of Chemically Modified DNA and Nucleic Acid Drug Targets

Joseph Larkin,[a] Spencer Carson,[a] Daniel H. Stoloff,[a] and Meni Wanunu*[a]

Abstract: Nucleic acids are central figures in many of life's key molecular processes, e.g., enzymatic activity, epigenetics/gene regulation, viral replication, aging, cancer, and other diseases. Over the past two decades, nanopores have emerged as a new tool for studying the properties of nucleic acids at the single-molecule level. In this review, we summarize the use of nanopores as sensors of nucleic acid structure, particularly for studying chemically modified and damaged DNA, and for probing the interactions of small-molecule drugs with nucleic acid targets.

Keywords: DNA · drugs · nanopores · RNA · single-molecule studies

1 Introduction

Apart from carrying inheritable genetic information, nucleic acids play tremendously diverse roles that are of prime contemporary interest in society. Nucleic acids are central in key topics such as viral pathogenicity, epigenetics, DNA damage and cancer, gene regulation, and ribosomal structure/function. Exploring the exact roles of nucleic acids with specific functions can point to new nucleic acid drug targets, as well as suggest mechanisms for disease.

A common structural feature in all nucleic acids is that under physiological conditions their phosphate-sugar backbone is negatively charged. This universal property leads to nucleic acid migration in the presence of an electric field. When a single nanopore in an ultrathin membrane is placed in the path of the migrating nucleic acids, individual nucleic acids are forced to translocate through the nanopore, one molecule at a time. By proper design of the nanopore dimensions, the electrolyte solution, and the electric field magnitude, the interactions of various nucleic acid molecules produce distinct electrical signatures that help to characterize their molecular structure. In just under two decades of research, the field of making various types of nanopores for studying nucleic acids has flourished.

In this review, we highlight some recent applications of various nanopore types for studying epigenetic DNA modifications, nucleic acid/drug complexes, and chemically damaged DNA. As will become evident in the text, the principal advantages of nanopores include the sensitivity to small DNA amounts (critical for epigenetic modification and damaged DNA analysis), submolecular resolution, and the ability to study unmodified nucleic acids, i.e., no chemical modification with fluorescent labels or surface-tethering groups is necessary. Future maturation of the nanopore technique as a commonplace analytical tool for nucleic acid studies can address challenges in both the clinical and research arenas.

2 Nanopore-Based Nucleic Acid Measurements

The basic principle of nanopore sensing is as follows. Figure 1a shows a side view of a nanoscale pore in an ultrathin membrane. The scheme is not drawn to scale, and the electrodes can be imagined as being a large distance away from the membrane (in practice, the membrane-electrode distance is typically 1–10 mm). The pore can either be a protein channel inserted into a lipid membrane, or a pore that is fabricated in a synthetic membrane material. While the pore type varies between different studies, the mechanism of nucleic acid detection is similar in all cases, relying on electrolyte flow for signal. Briefly, application of voltage across the membrane using a pair of electrodes results in a steady ion flow through the nanopore, providing a baseline current that is stable over time. The electric field profile that results from the bias across the membrane is shown in a color plot in Figure 1b. When large, charged macromolecules diffuse to the vicinity of the pore, the electric field (indicated by the color gradient) electrophoretically pulls the molecules into the pore, resulting in translocation. During passage

[a] J. Larkin, S. Carson, D. H. Stoloff, M. Wanunu
Department of Physics and Department of Chemistry and Chemical Biology
Northeastern University
Boston MA 02115 (USA)
e-mail: wanunu@neu.edu

Joseph Larkin finished his B. S. in Physics at Stanford University in 2007, and his M. S. in Physics at Boston University in 2012. He is currently a Ph.D. student in Meni Wanunu's lab at Northeastern. His research concerns incorporating solid-state nanopores into zero-mode waveguides to improve single-molecule real-time sequencing.

Spencer Carson completed his undergraduate studies at Gordon College in Wenham, Massachusetts, where he earned a Bachelor of Science (Physics, Mathematics) in May 2010. He started his Ph.D. education at Northeastern in August 2010 and received a Master of Science (Physics) in January 2012. Spencer has been working towards a Ph.D. in the lab of Dr. Meni Wanunu since joining in March 2012. His current research involves single-molecule experiments that sense the secondary structures of DNA and RNA using solid-state nanopores.

Daniel Stoloff obtained his B. S. in Physics from SUNY Buffalo. He joined Dr. Wanunu's group in 2011, with a research focus on nucleic acid interactions with solid-state nanopores.

Meni Wanunu completed his Ph.D. in 2005 at the Weizmann Institute of Science, where he specialized in supramolecular chemistry, self-assembly, and nanomaterials science. He then carried out a postdoctoral position at Boston University and a research associate position at the University of Pennsylvania, where he developed ultrasensitive synthetic nanopores for nucleic acid analysis at the single-molecule level. Currently, he is an Assistant Professor in the Department of Physics and the Department of Chemistry and Chemical Biology at Northeastern University, Boston. His research interests include developing chemical approaches for investigating biomolecular structure and behavior, nucleic acid mechanics and dynamics, and probing biological processes at the single-molecule level.

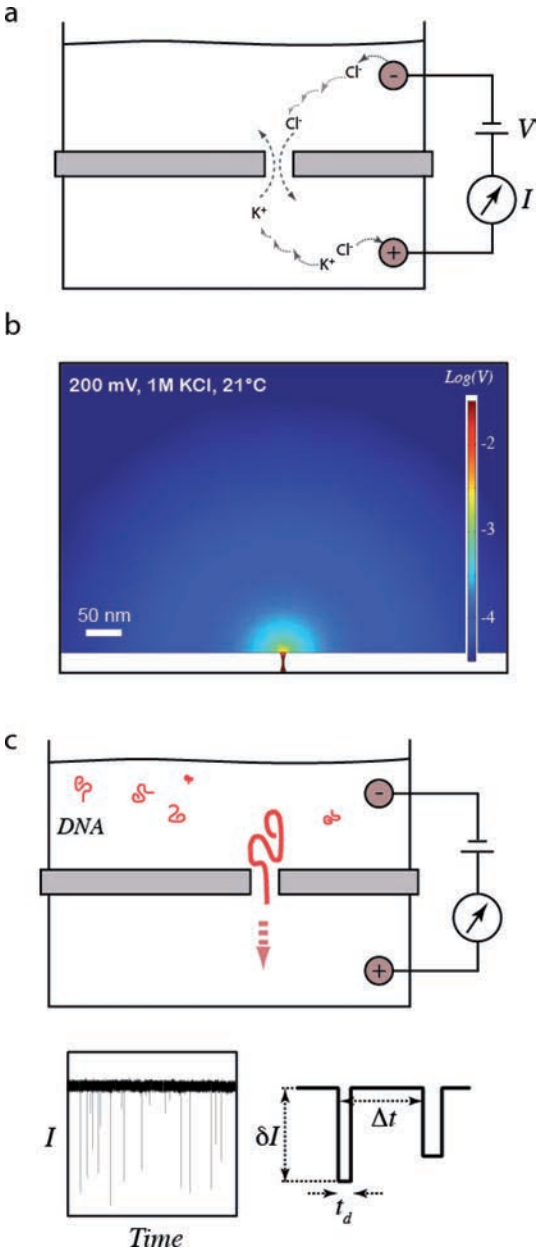

Figure 1. Nanopore measurement of biological macromolecules. a) Scheme of a nanopore setup for measurement of macromolecules. When voltage is applied, ion countercurrent generates a baseline current that is stable over time. b) Color map plot of a finite-element COMSOL simulation of a 4 nm pore in a 25 nm thick membrane, under the experimental conditions as outlined in the figure. Only the top chamber of the nanopore is shown. The electric field is visible as a color gradient, which is localized near the pore mouth. c) Ion current trace of double-stranded DNA molecule transport through a nanopore, along with the relevant quantities that are measured in the experiment. Schemes a) and c) are taken from reference [1].

of a molecule through the pore, the ion flow is transiently blocked, which provides a resistive spike that can be analyzed to study the molecule's properties (Figure 1c). Typi-

Israel Journal of Chemistry

cal analysis of single-molecule nanopore data includes statistical analysis of the mean pulse duration (t_d), mean blocked current (δI), and delay between successive events (Δt) for datasets of ~10^3 resistive pulses per experiment. It has previously been shown that mean pulse durations increase with the length of a DNA molecule, mean blocked currents increase with the width of a molecule (broadly defined), and the delay between successive events decreases with increasing concentrations of molecules. Although most nanopore experiments are performed at high salinity (e.g., 1 M monovalent salt) to improve the signal quality, improvements in signal quality over recent years have enabled experiments at lower (~ 0.2 M) salt concentrations.

3 Methylation as an Epigenetic Marker

Epigenetic markers in DNA have been observed in both prokaryotes and eukaryotes in the form of modified bases (chemically altered forms of the familiar A, T, C, and G).[2] A common modification found in about 5% of cytosines is methylation to form 5-methylcytosine (mC), which is most commonly seen in CpG regions of DNA.[3,4] The function of this methylation is not completely understood, but it has been suggested that it could play a major role in promoter regions, which in effect control gene expression.[5] The abnormal methylation of these CpG islands has been shown to overly silence or activate transcription in these promoter regions, which is implicated in many types of cancer.[6,7] Understanding and locating the patterns of methylation as biomarkers of disease is the major motivation for easier detection of methylated DNA.

Although mC is the most common epigenetic marker in DNA, another was found in 1972 by Penn[8] and later confirmed in 2009.[9,10] Often referred to as the "sixth base", 5-hydroxymethylcytosine (hmC) was found in mammalian Purkinje cells and embryonic stem cells.[9] It has been especially challenging to distinguish between 5-methylcytosine and 5-hydroxymethylcytosine due to their subtle structural differences (see Figure 2a). Typically, bisulfite sequencing is the most common chemical assay for identifying methylation patterns in DNA,[11] but its downfall is that it cannot differentiate between mC and hmC as both altered bases prevent the bisulfite-aided oxidation of cytosine to uracil. Another popular method of distinguishing C and mC is digesting DNA with methylation-dependent restriction enzymes,[3] but again this cannot distinguish between mC and hmC since both modified bases hamper the activity of the enzymes. These difficulties make using nanopores particularly advantageous because observing the changes in the pore current can potentially sense these slight variations in structure.

The differences in C and mC have been well observed by the use of alpha-hemolysin (αHL) pores[12,13] and solid-state SiN nanopores.[14,15] Since tranlocation across αHL is too fast for individual base resolution (1–3 μs per base)[16] in an ssDNA strand, an exonuclease is used to unselectively cut the ssDNA samples into dNMPs. These individual bases were translocated through the nanopore and the residual current measured by these experiments indicated that mC blocks more ion flow than C, which is expected due to the extra methyl group.[13] This achievement was useful, but differentiation between C and mC is also possible by standard methods like bisulfite sequencing.[11]

By binding a streptavidin-biotin complex to intact ssDNA samples, Wallace and coworkers were able to distinguish between all types of cytosine by capturing an ssDNA complex and reading a specific location multiple times (see Figure 2d).[12] Another strategy is to use solid-state nanopores to detect synthetic dsDNA (400 bp and 3000 bp) with only C, mC, or hmC bases and to note the changes in both residual current and dwell time of translocation events (see Figure 2b and 2c).[14] It was found in the studies described above that the three bases were noticeably distinct according to their current blockage and dwell time properties. More specifically, it was noted that the dwell times followed the trend hmC > C > mC, which is not what would be expected based on the molecular sizes. It was theorized and confirmed that this result is due to the hydrophobicity of mC, which causes the DNA to be less flexible and therefore results in shorter dwell times compared to C and hmC.[14] Once nanopore transport is slowed down and understood more fully this technology could be used to analyze the epigenome of any given mammalian DNA sample without bisulfite sequencing or DNA amplification.

4 Sensing G-Quadruplex Structures

Nanopores can be employed to study tertiary structures of DNA outside of the standard Watson-Crick double helix. One structure of particular interest is the G-quadruplex, which forms in guanine-rich sequences and is most commonly found in telomeres,[21,22] single-stranded sequences of DNA at the ends of chromosomes, and gene promoter regions.[23,24] The consistent motif of G-quadruplex formation is the stacking of G-quartets, which are stabilized by monovalent or bivalent cations, with loops of one to seven bases interconnecting these guanine sections (see Figure 3a and 3b).[19,25] When it was found in the mid-1990s that cellular immortalization was catalyzed by telomerases in roughly 85% of cancer cells, scientists sought methods for inhibiting its activity.[26] Later, it was proposed that quadruplexes could also form in genomic DNA sequences and these have been characterized extensively by x-ray diffraction[27] and NMR studies.[18] In the case of both telomeric and genomic sequences it was desired to stabilize the G-quadruplex by binding small

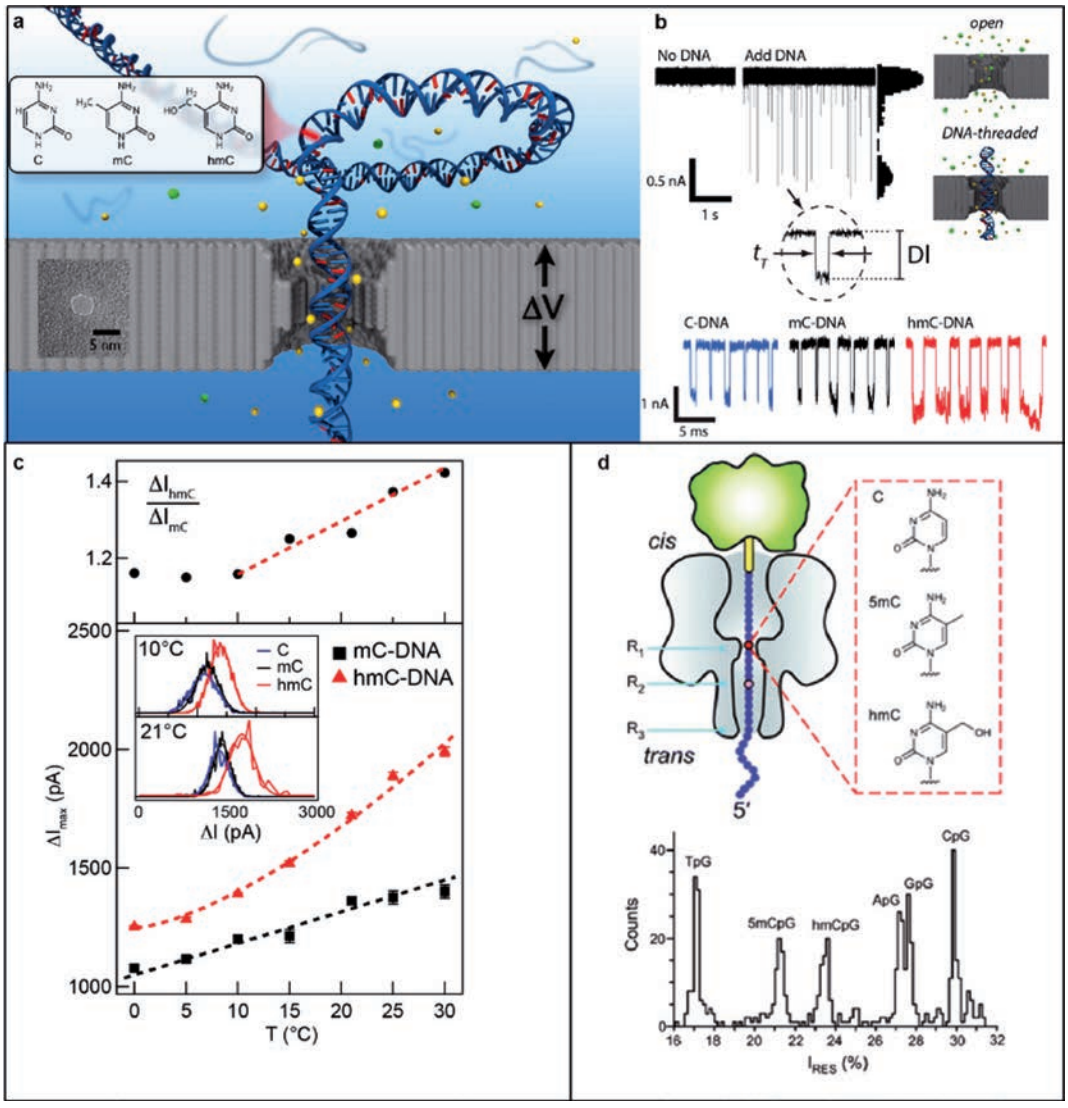

Figure 2. Detection of modified DNA bases. a) Schematic of dsDNA translocating through a 4 nm solid-state nanopore as shown by inset TEM image.[14] The chemical structures of cytosine and the modified bases 5-methylcytosine (mC) and 5-hydroxymethylcytosine (hmC) are also shown. b) Top: sample current traces for the nanopore with and without DNA are shown. Bottom: concatenated current traces for experiments involving 3 kbp DNA exclusively containing C, mC, or hmC. As evidenced by the events, the three DNA bases cause varying transport characteristics for both dwell time and current blockage. c) The temperature dependence of current blockage for mC-DNA and hmC-DNA. Both specimens show an increase in ΔI when temperature is increased, but hmC increases by a greater factor. Inset: the histograms of ΔI demonstrate the increased pore blockage of hmC-DNA compared to C-DNA and mC-DNA at bath temperatures of 10° and 21°.[14] d) An ssDNA-biotin-streptavidin complex is immobilized in an α-hemolysin nanopore by an applied voltage. Each base modification has a signature residual current, as evidenced by the distinct peaks.[12]

molecules in order to repress the activity of DNA polymerases.[28–30]

Several studies have shown that the formation of G-quadruplexes in ssDNA can be sensed using αHL nanopores to determine properties such as folding/unfolding kinetics, cation dependencies, and G-quadruplex interactions.[20,31,32] Shim et al. demonstrated that a particular DNA oligonucleotide (GGTTGGTGTGGTTGG) can form a G-quadruplex in various electrolytic solutions and found that the stability and folding kinetics are salt dependent (see Figure 3c).[20] One can determine structural traits by other methods, such as atomic force microscopy[33,34] and fluorescence resonance energy transfer (FRET) spectroscopy,[35] but nanopores are preferable since there is no need for the labeling or immobilization of DNA to obtain information. Based on the number and types of nucleotides contained in loops that connect the G-quartets, there are as many as 26 theoretical conformations possible for the folding of a G-quadruplex.[36] Due to the variance of these topologies, it seems probable that

Israel Journal of Chemistry

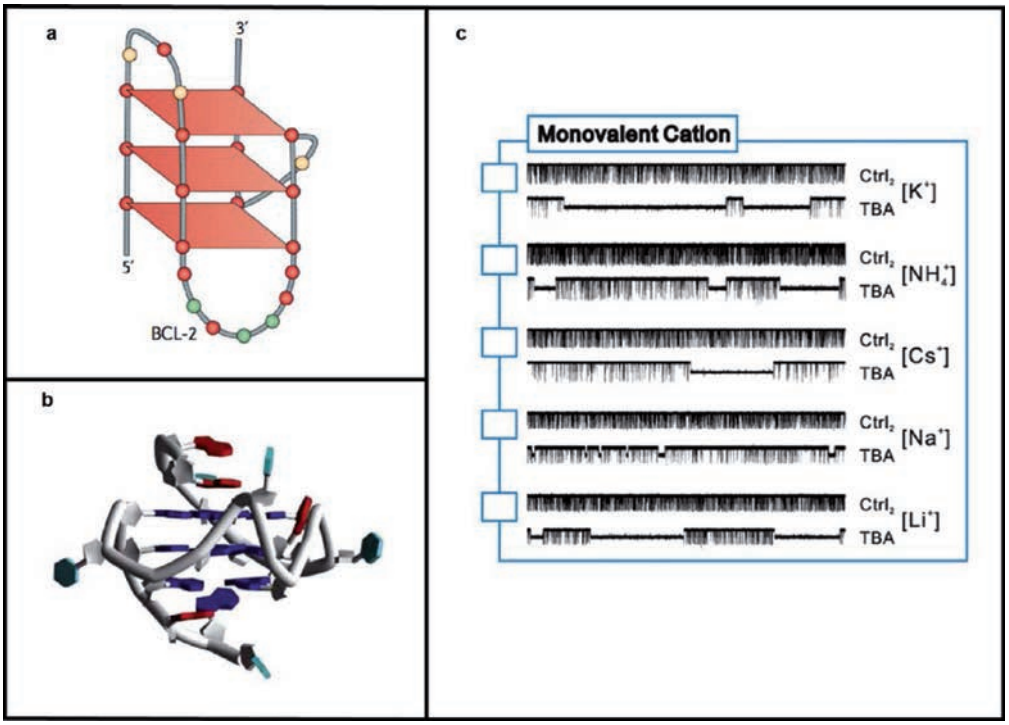

Figure 3. G-quadruplex geometry and cation preferences. a) A "ball-and-chain" model of the G-quadruplex conformation found in B-cell lymphoma (BCL-2).[17] The stacked G-quartets are connected by loops of length three, seven, and one bases. b) A 3-D rendition of G-quadruplex folding often found in the C-MYC promoter region (PDB ID: 1XAV),[18] in which guanine bases are in dark blue, adenine bases are in red, and thymine bases are in cyan.[19] c) Translocation events using α-hemolysin for thrombin-binding aptamer (TBA), a G-rich 15-mer known to fold into a compact quadruplex, and control 15-mer DNA samples ($Ctrl_2$). In contrast to $Ctrl_2$, TBA produces a few events that are much longer than typical ssDNA translocations for all the 1 M monovalent salt solutions attempted (K^+, NH_4^+, Cs^+, Na^+, and Li^+), which signifies the presence of quadruplex formation.[20]

in future work nanopores may be able to distinguish subtle changes in quadruplex diameter and kinetics. Although it has been shown that G-quadruplexes will form in coding strands of dsDNA, it has not been confirmed experimentally that this tertiary structure is favorable enough to exist in duplex DNA.[37] Given the proper conditions (i.e., pH, salt concentration, and temperature), it is possible that solid-state nanopores could sense the presence of G-quadruplexes due to differences in the diameters of double helix dsDNA and G-quadruplex/i-motif DNA.

5 Probing Nucleic Acid/Drug Interactions

The interactions between drugs and nucleic acids or proteins are of incredible value for research and clinical purposes. Current methods of study can lack sensitivity or speed, or necessitate large quantities of the molecule for detection. Furthermore, most methods involve chemical labeling that can often disrupt the native biomolecular structure, lowering the applicability and veracity of results. Because nanopores are label free, real time and very sensitive at even very low concentrations, they are a promising tool for a wide variety of drug interaction studies.

As a proof of concept, the intercalation of molecules into DNA was studied using a solid-state nanopores (Figure 4). Intercalation of molecules into nucleic acids involves a molecule able to bind itself between base pairs, expanding the diameter of the nucleic acids. In a double-stranded DNA fragment, ethidium bromide was found to intercalate to the DNA causing a swelling in DNA diameter, which corresponds to a larger current blockage during translocations. The deepening of blockages was found to increase with the amount of ethidium bromide added, allowing for an accurate measurement of its dissociation constant. Using a smaller solid-state nanopore, the intercalation of SYBR Green II (SGII) to single-stranded DNA was investigated. SGII is a cyanine dye that binds with high affinity to random single-stranded sequences of DNA. In the presence of SGII, much deeper current blockages were found for translocation than when there was no dye present. As a further proof, a selected sequence of DNA containing one repeated base was found by other methods to have very low affinity for binding with SGII. In the nanopore there was no change in translocation signature after the introduction of SGII.[38]

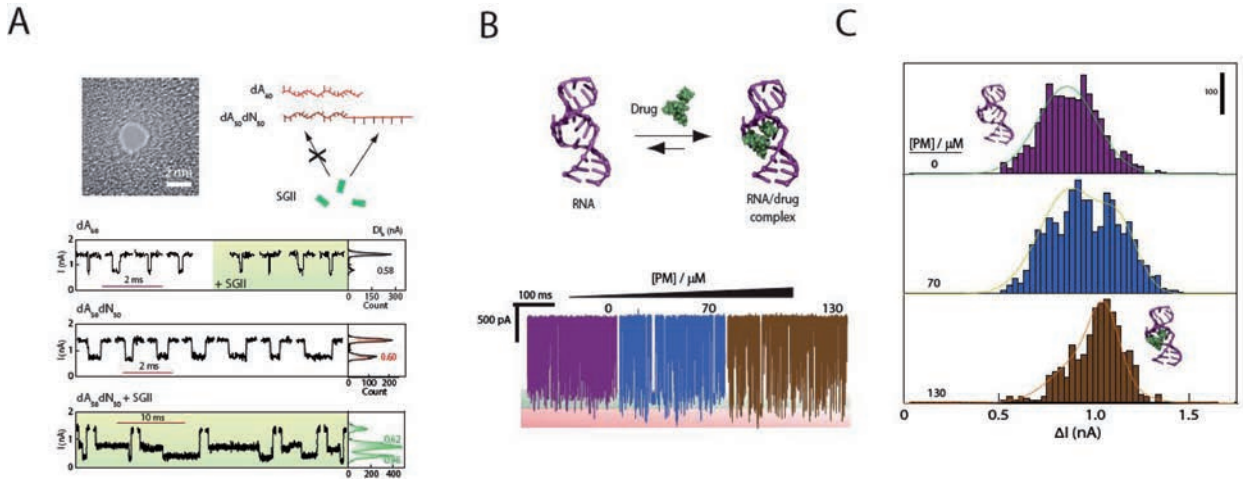

Figure 4. Small-molecule binding to DNA and RNA. a) Transmission electron microscope image of a 2.2 nm pore, alongside a cartoon of single-stranded DNA and cyanine dye SYBR Green II. SGII binds with very low affinity to repeated bases, labeled as dA_{60}, but binds with high affinity to a random sequence, labeled $dA_{50}dN_{50}$. Below are sample current traces for different molecules interacting with the nanopores, showing the behavior of the molecules during translocation. There is no observable change when SGII is introduced to the low binding affinity dA_{60}, but a marked change in the currents occurs when introduced to the high binding affinity $dA_{50}dN_{50}$.[38] b) A cartoon of the RNA/drug-complex formation. Current traces are shown for different drug concentrations. c) A histogram of current blockages for the different drug concentrations is shown. The current blockage increases as more drug is added, correlating with the expansion of the molecule due to drug binding.[39]

Antimicrobial binding to RNA molecules is of great importance for the treatment of bacterial and viral infections. A target for these antibiotic bindings is the prokaryotic ribosomal RNA decoding site, usually called the A-site. Studies using other single-molecule techniques, such as FRET, have found that the area has a high-affinity binding. Using a 3.5 nm solid-state nanopore, the binding of different antibiotics was observed by a deepening of current blockage values. Using different antibiotics with different binding affinities, the specific differences in drug binding were observed, showing high agreement with other methods. The effect of the salt concentration in the solution was also shown to create an observable change in binding affinity, another result that agrees strongly with previous literature.[39]

The function and structure of a biomolecule can be significantly modified when in the presence of a binding chemical structure. This change can be exhibited as a large-scale change in tertiary structure, which is a valuable target for the detection and study of illicit drugs. For example, a single-stranded DNA aptamer was found to undergo a large structural change when cocaine binds to it (Figure 5a). The unbound aptamer is capable of translocation in an αHL biological pore. When cocaine is injected into the molecule, a large tertiary structure is formed that prevents translocation, causing the nanopore to clog. By then expelling the molecule with a reversed bias, Kawano was able to find the concentration of molecules that had formed drug-bound structures. They were able to detect the presence of 3 μg/mL of cocaine in 25 s, a much smaller and faster detection than many current methods.[40]

αHL pores were also able to probe an important relationship between methamphetamine and Parkinson's disease. The protein chain alpha-synuclein is abundant in dopaminergic neurons and is believed to play a role in a variety of neurological disorders, including Parkinson's disease. An observed relationship between a higher rate of Parkinson's disease in methamphetamine users made the interaction of the drug with alpha-synuclein worthy of investigation. The Lee group found that alpha-synuclein would translocate across an αHL pore, but as the amount of methamphetamine was added translocations became less likely as much lower current blockages began to occur (Figure 5b). This is believed to be due to a looping behavior formed by the binding of alpha-hemolysin, with the loop being much larger than the pore opening. This result could prove to be very important in treatment and detection of other neurological disorders, as this behavior is likely to occur for other chemical structures besides methamphetamine.[41]

6 Detecting Damaged DNA with α-Hemolysin

Oxidative stress can damage DNA in several ways. Guanine is the most easily ionized nucleotide. Radicals, genotoxins, and ultraviolet radiation may convert guanine to the damaged base 8-oxo-7,8-dihydroguanine (OG).[42] Excessive oxidative damage has been found in the cellular DNA of many tumor samples, suggesting that oxidized

Israel Journal of Chemistry

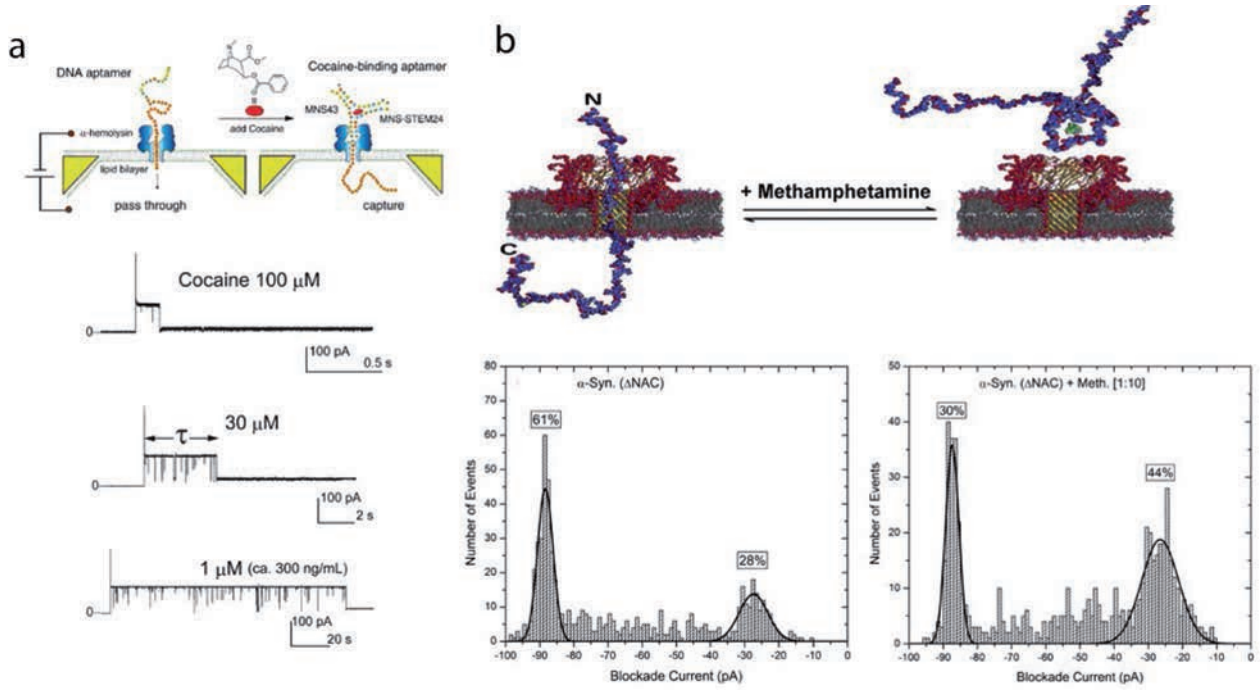

Figure 5. Detection of small-ligand binding. a) A DNA aptamer forms a structure in the presence of cocaine that is several times the width of an alpha-hemolysin pore, so that translocations become impossible. The basic schematic is shown, with sample traces in the presence of different concentrations of cocaine. The time before a long blockage occurs corresponds strongly with the concentration of cocaine, which renders this approach a high-throughput, low-concentration detection scheme.[40] b) The alpha-synuclein protein chain, an important neurological protein, is believed to form a loop in the presence of methamphetamine. Histograms of current blockages show an increase in shallow blockages, corresponding to molecules that are incapable of translocation, as methamphetamine is added, in accordance with the proposed loop behavior.[41]

DNA may play a role in carcinogenesis. Furthermore, DNA oxidation may lead to a variety of nervous system, liver, and cardiovascular diseases.[43] Once oxidized, OG is susceptible to further oxidation into a variety of products.[44,45] Repairs to damaged sites and spontaneous hydrolysis of glycosidic bonds can result in a separate form of damage called an apurinic/apyrimidinic (AP) or abasic site. AP sites are spots along a DNA strand with no purine or pyrimidine base group at all.[46] In addition to mutations, AP sites can in fact cause structural DNA damage like single-strand breaks and DNA cross-linking.[47] Improved detection of these lesions clearly has valuable application in medicine and medical research. Figure 6a shows the structure of OG, two of its further-oxidized products, and an AP site.

Bulk techniques including the comet assay and HPLC combined with mass spectrometry have traditionally detected oxidative damage in DNA.[48] These approaches either overestimate the degree of damage or require enzymatic processing of samples prior to detection. Moreover, none of the bulk tools offer sequence information, nor discriminate between single oxidized sites and multiple-site damage.[49,50] The stability of DNA complexes with oxidized sites and their unzipping or dissociation kinetics have also been studied with a variety of tools. Thermodynamic models accurately predict melting temperatures for damaged DNA molecules, but give no kinetic information. Atomic force microscopy and optical tweezers can give single-molecule kinetic information, but require extensive chemical modification of samples and force probes.[51] AP sites have been studied with a similar variety of bulk techniques, but the field lacks single-molecule tools that give sequence information.[52]

Many of the problems with measuring DNA damage can be alleviated by studying damaged molecules with αHL nanopores. White and Burrows have published extensive studies of damaged DNA with αHL in lipid membranes.[49–52] Conjugating biotinylated ssDNA fragments with streptavidin allows an αHL in a biased membrane to trap DNA fragments.[53–55] Because the streptavidin is too large to fit into the pore vestibule, the molecule will sit trapped in the pore while the voltage bias is on. Monitoring the current through the pore gives information about the interaction of the sample DNA with the residues of the αHL barrel. The nucleotide at the 14th position relative to the 3′-end of the ssDNA fragment interacts most strongly with the αHL pore.[53] Synthesizing an ssDNA with an OG, or the subsequent oxidative products spiroiminodihydantoin (Sp) or guanidinohydantoin (Gh), at position 14 allows single-molecule αHL probing of the oxi-

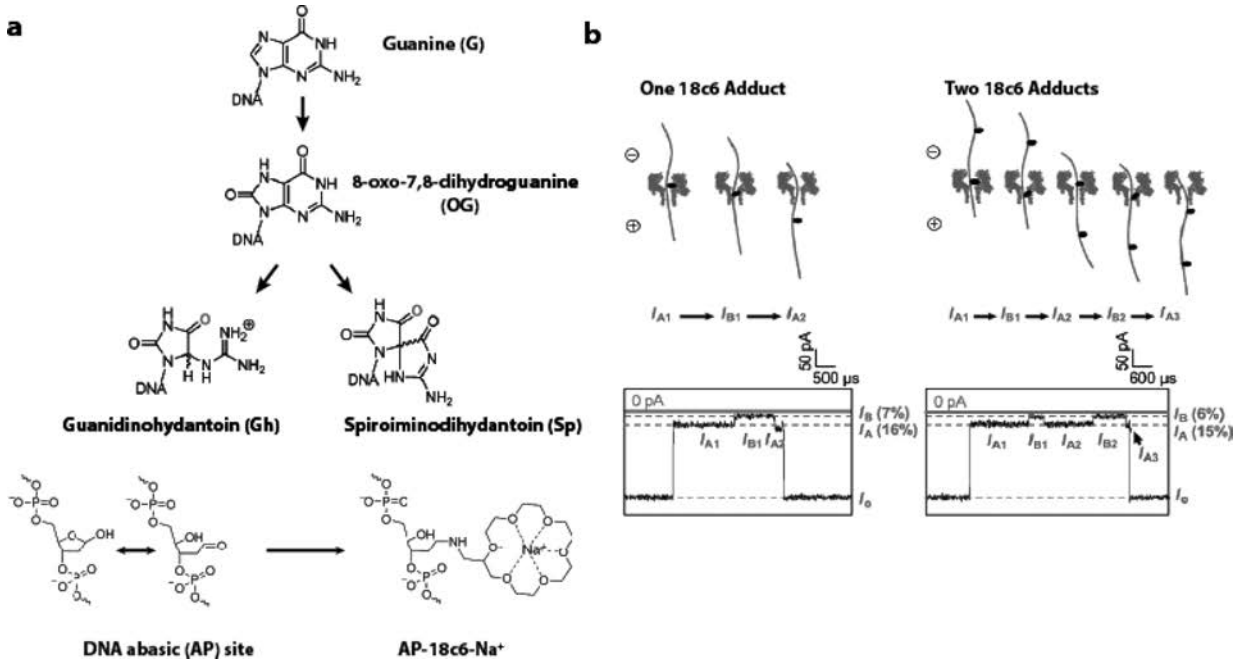

Figure 6. a) The structures of the various damaged bases studied is shown. Guanine (G) may be oxidized to 8-oxo-7,8-dihydroguanine (OG), which forms slightly less stable hydrogen bonds than G and may be further oxidized to the highly destabilizing groups guanidinohydantoin (Gh) and spiroiminodihydantoin (Sp). The bottom row illustrates the structure of an AP site, and the structure of the bulky 18-crown-6 group (18c6) used for labeling AP sites. b) Translocation of ssDNA with one or two 18c6-labeled AP sites is shown to have multiple current blockage levels, the deeper current blockage level (I_B) of the bulky groups and the lower blockage of bare ssDNA (I_A).

dized DNA. Immobilizing such a complex in a nanopore shows that an OG site blocks nearly the same current as a G, whereas Gh generally blocks less than G and Sp more, with both Gh and Sp displaying wider distribution of current blockage than either G or OG.[49] Positioning the damaged bases in a genomic sequence instead of a homogeneous poly(dC) background changes the interaction of the damaged DNA with the nanopore, allowing clear discrimination between G, OG, Sp, and Gh current blockage levels.[49] This technique is not unlike that used to detect different methylated bases, as discussed earlier in this review.

A similar experiment enables detection of an AP site on a single ssDNA molecule. The AP site allows selective attachment of a bulky 18-crown-6 (18c6) group to the important 14th position along the DNA. Upon entry of this molecule into the pore, one can observe an initial current blockage level (I_A) corresponding to the ssDNA entering the pore. In certain events, after some time the current drops to a 4.6% deeper blockage level (I_B). I_B corresponds to the 18c6 sitting at the most sensitive position of the pore. In addition to this two-level state, it is also possible to see the current go straight from open-pore level to I_A or I_B. The different blockage levels correspond to different states of the AP-18c6 molecule. At the I_B level, the experimenters hypothesize that the 18c6 adduct is in its most compact conformation, allowing it to enter the narrow pore vestibule. This hypothesis is supported by the fact that the two-level events are not seen when the ssDNA enters the pore from the 3′-end. Instead, the vast majority of 3′-entry events display immediate blocking to the deep I_B level. When the ssDNA enters from the 3′-end, it experiences less friction with the pore than when it enters from the 5′-end.[56] The 18c6 group is then sterically hindered when the strand enters from this end, and some time is required for the 18c6 to adopt the appropriate conformation, enter the pore constriction, and block the current to the I_B level. 3′-entry results in less friction and lower steric hindrance of the 18c6, so it can quickly adopt the narrower constriction, and immediately block the pore to I_B upon entry.[52]

By translocating an ssDNA molecule with 18c6-labeled AP sites, one can detect multiple AP sites on one molecule. The same group that conducted the above studies also translocated two different damaged ssDNA molecules. One had a single 18c6-labeled AP site and the other two labeled AP sites 35 nucleotides apart. The scheme of this experiment is depicted in Figure 6b. In these translocation experiments, like in the streptavidin-biotin immobilization, the 18c6-adducted DNA can block current to two different levels, I_A and I_B. As one might expect, the strand with only one 18c6 displays one pulse of I_A to I_B blockage during translocation, and the doubly labeled molecule consistently shows two I_B pulses (Fig-

Israel Journal of Chemistry

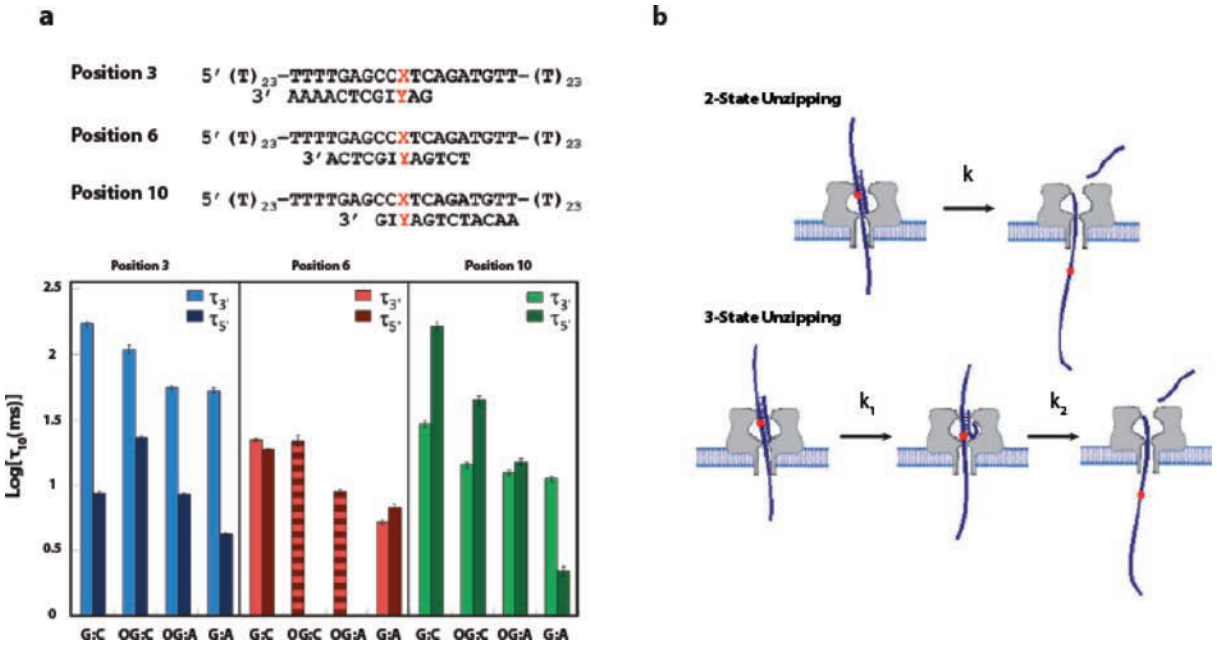

Figure 7. a) The oxidative lesion was placed at three different locations along a duplex region to be unzipped. By comparing the difference between 3′ (lighter) and 5′ (darker) unzipping times, the experimenters can differentiate samples with different damaged locations along the molecule. b) G and OG fit a two-state unzipping model, Gh and Sp a three-state unzipping model. The red dot corresponds to the location of the oxidized base.

ure 6b).[52] Using this technique, the αHL nanopore can differentiate ssDNA molecules with one AP site from those with two sites only 35 nucleotides apart. The closeness of the two AP sites along the DNA strand is limited by the length of the pore, because to detect two molecules, they must be at least far enough apart so that one AP site is completely through the pore before the next site enters.

An important application of translocation is unzipping double-stranded DNA. Because the αHL pore is too narrow to accommodate dsDNA in its barrel, threading a dsDNA with a short single-stranded overhang into the pore allows the voltage bias to dissociate the shorter DNA strand and translocate the longer strand. By repeatedly measuring the duration of the current blockade for this process, one can extract the single-molecule kinetics of a nanopore unzipping a DNA molecule.[57] Unsurprisingly, White, Burrows, and their groups have performed the key experiments applying this technique to damaged DNA. OG forms hydrogen bonds with cytosine at nearly the same stability as does G, and can even form semi-stable hydrogen bonds with adenine.[58] White and Burrows unzipped a 65-mer ssDNA with a 10-mer duplex region in the middle of the molecule. By examining the distribution of unzipping times, they differentiated populations of samples containing a single G:C, OG:C, G:A, and OG:A pair in the 10-mer double-stranded region. They also distinguished between three different positions of the OG site by moving it along the 10-mer region and examining the resulting difference in unzipping times for 3′- and 5′-entry into the pore.[50] Figure 7a depicts the three different damage locations and the means by which their locations are discerned via unzipping. This data offers the discrimination of oxidative damage location that bulk methods cannot achieve.

While OG forms stable hydrogen bonds with a complementary base, its further oxidative products, Sp and Gh, do not.[59] The White and Burrows groups measured the kinetics of unzipping dsDNA with these particular lesions. The sample molecule is a 17-mer DNA strand bound to a 65-mer with a complementary region in the middle. In the center of the duplex, the experimenters put either a G:C, OG:C, Sp:C, or Gh:C pair. They then performed αHL unzipping experiments with these molecules. In addition to finding unzipping times one to two orders of magnitude faster for the molecules with the less stable Sp:C or Gh:C pairing, the distribution of unzipping times for these further oxidized lesions fits a different unzipping model altogether. The G:C and OG:C unzipping time distributions fit a two-state model of unzipping kinetics. The first state corresponds to the duplex region being intact in the pore, the second state to the 17-mer being completely dissociated. Fitting the unzipping times for G and OG to such a model, White and Burrows et al. extracted unzipping rates, with the OG unzipping rate a factor of four greater than that of G. The distribution of Sp and Gh unzipping times, however, fits a three-state model. The first state corresponds to the intact duplex, the second to the duplex being dissociated from one end up to the lesion site, and the third being a completely dissociated 17-mer.

Figure 7b illustrates the two different unzipping models. Upon fitting the unzipping times to this three-state model, the Sp and Gh sites each have two different unzipping rates, both of which are one to two orders of magnitude faster than the unzipping rates for G and OG.[51]

7 Summary and Outlook

Nanopores are promising new tools for studying unlabeled nucleic acid molecules in solution. In this review we have covered the use of nanopores for studying DNA epigenetic modifications, damaged DNA molecules, DNA tertiary structures, and nucleic acid–ligand interactions. In just under a decade, many reports have conveyed the relevance and convenience of using nanopores for single-molecule studies of nucleic acid structure. Future development of nanopore devices that offer long lifetimes, reproducible structures, and convenient handling would further aid in the adoption of the nanopore technique for various non-specialized research and clinical laboratories worldwide.

References

[1] M. Wanunu, *Phys. Life Rev.* **2012**, *9*, 125–158.
[2] J. H. Gommersampt, P. Borst, *FASEB J.* **1995**, *9*, 1034–1042.
[3] R. Brena, T.-M. Huang, C. Plass, *J. Mol. Med.* **2006**, *84*, 365–377.
[4] S. Beck, V. K. Rakyan, *Trends Genet.* **2008**, *24*, 231–237.
[5] J. G. Herman, S. B. Baylin, *N. Engl. J. Med.* **2003**, *349*, 2042–2054.
[6] S. A. Qureshi, M. U. Bashir, A. Yaqinuddin, *Int. J. Surg.* **2010**, *8*, 194–198.
[7] P. W. Laird, *Nat. Rev. Cancer* **2003**, *3*, 253–266.
[8] N. W. Penn, R. Suwalski, C. O'Riley, K. Bojanowski, R. Yura, *Biochem. J.* **1972**, *126*, 781–790.
[9] S. Kriaucionis, N. Heintz, *Science* **2009**, *324*, 929–930.
[10] M. Tahiliani, K. Peng Koh, Y. Shen, W. A. Pastor, H. Bandukwala, Y. Brudno, S. Agarwal, L. M. Iyer, D. R. Liu, L. Aravind, A. Rao, *Science* **2009**, *324*, 930–935.
[11] H. Hayatsu, *Mutat. Res., Rev. Mutat. Res.* **2008**, *659*, 77–82.
[12] E. V. B. Wallace, D. Stoddart, A. J. Heron, E. Mikhailova, G. Maglia, T. J. Donohoe, H. Bayley, *Chem. Commun.* **2010**, *46*, 8195–8197.
[13] J. Clarke, H.-C. Wu, L. Jayasinghe, A. Patel, S. Reid, H. Bayley, *Nat. Nanotechnol.* **2009**, *4*, 265–270.
[14] M. Wanunu, D. Cohen-Karni, R. R. Johnson, L. Fields, J. Benner, N. Peterman, Y. Zheng, M. L. Klein, M. Drndic, *J. Am. Chem. Soc.* **2011**, *133*, 486–492.
[15] U. Mirsaidov, W. Timp, X. Zou, V. Dimitrov, K. Schulten, A. P. Feinberg, G. Timp, *Biophys. J.* **2009**, *96*, L32–L34.
[16] A. Meller, L. Nivon, E. Brandin, J. Golovchenko, D. Branton, *Proc. Natl. Acad. Sci. U.S.A.* **2000**, *97*, 1079–1084.
[17] S. Balasubramanian, L. H. Hurley, S. Neidle, *Nat. Rev. Drug Discovery* **2011**, *10*, 261–275.
[18] A. Ambrus, D. Chen, J. Dai, R. A. Jones, D. Yang, *Biochemistry* **2005**, *44*, 2048–2058.
[19] S. Neidle, *Curr. Opin. Struct. Biol.* **2009**, *19*, 239–250.
[20] J. Shim, L.-Q. Gu, *Methods* **2012**, *57*, 40–46.
[21] W. I. Sundquist, A. Klug, *Nature* **1989**, *342*, 825–829.
[22] S. Neidle, G. N. Parkinson, *Curr. Opin. Struct. Biol.* **2003**, *13*, 275–283.
[23] T. Simonsson, M. Kubista, P. Pecinka, *Nucleic Acids Res.* **1998**, *26*, 1167–1172.
[24] A. Siddiqui-Jain, C. L. Grand, D. J. Bearss, L. H. Hurley, *Proc. Natl. Acad. Sci. U.S.A.* **2002**, *99*, 11593–11598.
[25] S. Burge, G. N. Parkinson, P. Hazel, A. K. Todd, S. Neidle, *Nucleic Acids Res.* **2006**, *34*, 5402–5415.
[26] D. Sun, B. Thompson, B. E. Cathers, M. Salazar, S. M. Kerwin, J. O. Trent, T. C. Jenkins, S. Neidle, L. H. Hurley, *J. Med. Chem.* **1997**, *40*, 2113–2116.
[27] G. N. Parkinson, M. P. H. Lee, S. Neidle, *Nature* **2002**, *417*, 876–880.
[28] J. Seenisamy, E. M. Rezler, T. J. Powell, D. Tye, V. Gokhale, C. S. Joshi, A. Siddiqui-Jain, L. H. Hurley, *J. Am. Chem. Soc.* **2004**, *126*, 8702–8709.
[29] S. M. Gowan, J. R. Harrison, L. Patterson, M. Valenti, M. A. Read, S. Neidle, L. R. Kelland, *Mol. Pharmacol.* **2002**, *61*, 1154–1162.
[30] B. Brassart, D. Gomez, A. De Cian, R. Paterski, A. Montagnac, K.-H. Qui, N. Temime-Smaali, C. Trentesaux, J.-L. Mergny, F. Gueritte, J.-F. Riou, *Mol. Pharmacol.* **2007**, *72*, 631–640.
[31] X. Hou, W. Guo, F. Xia, F.-Q. Nie, H. Dong, Y. Tian, L. Wen, L. Wang, L. Cao, Y. Yang, J. Xue, Y. Song, Y. Wang, D. Liu, L. Jiang, *J. Am. Chem. Soc.* **2009**, *131*, 7800–7805.
[32] J. W. Shim, Q. Tan, L.-Q. Gu, *Nucleic Acids Res.* **2009**, *37*, 972–982.
[33] Z. Kan, Y. Lin, F. Wang, X. Zhuang, Y. Zhao, D. Pang, Y. Hao, Z. Tan, *Nucleic Acids Res.* **2007**, *35*, 3646–3653.
[34] Y. Sannohe, M. Endo, Y. Katsuda, K. Hidaka, H. Sugiyama, *J. Am. Chem. Soc.* **2010**, *132*, 16311–16313.
[35] L. Ying, J. J. Green, H. Li, D. Klenerman, S. Balasubramanian, *Proc. Natl. Acad. Sci. U.S.A.* **2003**, *100*, 14629–14634.
[36] M. Webba da Silva, *Chem. Eur. J.* **2007**, *13*, 9738–9745.
[37] A. N. Lane, J. B. Chaires, R. D. Gray, J. O. Trent, *Nucleic Acids Res.* **2008**, *36*, 5482–5515.
[38] M. Wanunu, J. Sutin, A. Meller, *Nano Lett.* **2009**, *9*, 3498–3502.
[39] M. Wanunu, S. Bhattacharya, Y. Xie, Y. Tor, A. Aksimentiev, M. Drndic, *ACS Nano* **2011**, *5*, 9345–9353.
[40] R. Kawano, T. Osaki, H. Sasaki, M. Takinoue, S. Yoshizawa, S. Takeuchi, *J. Am. Chem. Soc.* **2011**, *133*, 8474–8477.
[41] O. Tavassoly, J. S. Lee, *FEBS Lett.* **2012**, *586*, 3222–3228.
[42] J. Cadet, T. Douki, J. L. Ravanat, *Acc. Chem. Res.* **2008**, *41*, 1075–1083.
[43] M. S. Cooke, R. Olinski, M. D. Evans, *Clin. Chim. Acta* **2006**, *365*, 30–49.
[44] W. Luo, J. G. Muller, E. M. Rachlin, C. J. Burrows, *Org. Lett.* **2000**, *2*, 613–616.
[45] Y. Ye, J. G. Muller, W. Luo, C. L. Mayne, A. J. Shallop, R. A. Jones, C. J. Burrows, *J. Am. Chem. Soc.* **2003**, *125*, 13926–13927.
[46] S. Boiteux, M. Guillet, *DNA Repair* **2004**, *3*, 1–12.
[47] K. S. Gates, *Chem. Res. Toxicol.* **2009**, *22*, 1747–1760.
[48] J. Cadet, H. Poulsen, *Free Radical Biol. Med.* **2010**, *48*, 1457–1459.
[49] A. E. P. Schibel, N. An, Q. Jin, A. M. Fleming, C. J. Burrows, H. S. White, *J. Am. Chem. Soc.* **2010**, *132*, 17992–17995.

Israel Journal of Chemistry

[50] A. E. P. Schibel, A. M. Fleming, Q. Jin, N. An, J. Liu, C. P. Blakemore, H. S. White, C. J. Burrows, *J. Am. Chem. Soc.* **2011**, *133*, 14778–14784.
[51] Q. Jin, A. M. Fleming, C. J. Burrows, H. S. White, *J. Am. Chem. Soc.* **2012**, *134*, 11006–11011.
[52] N. An, A. M. Fleming, H. S. White, C. J. Burrows, *Proc. Natl. Acad. Sci. U.S.A.* **2012**, *109*, 11504–11509.
[53] D. Stoddart, A. J. Heron, J. Klingelhoefer, E. Mikhailova, G. Maglia, H. Bayley, *Nano Lett.* **2010**, *10*, 3633–3637.
[54] R. F. Purnell, K. K. Mehta, J. J. Schmidt, *Nano Lett.* **2008**, *8*, 3029–3034.
[55] S. E. Henrickson, M. Misakian, B. Robertson, J. J. Kasianowicz, *Phys. Rev. Lett.* **2000**, *85*, 3057–3060.
[56] J. Muzard, M. Martinho, J. Mathé, U. Bockelmann, V. Viasnoff, *Biophys. J.* **2010**, *98*, 2170–2178.
[57] A. F. Sauer-Budge, J. A. Nyamwanda, D. K. Lubensky, D. Branton, *Phys. Rev. Lett.* **2003**, *90*, 238101.
[58] L. A. Lipscomb, M. E. Peek, M. L. Morningstar, S. M. Verghis, E. M. Miller, A. Rich, J. M. Essigmann, L. D. Williams, *Proc. Natl. Acad. Sci. U.S.A.* **1995**, *92*, 719–723.
[59] F. Chinyengetere, E. R. Jamieson, *Biochemistry* **2008**, *47*, 2584–2591.

Received: January 31, 2013
Accepted: March 29, 2013
Published online: June 5, 2013

